Magnetic field effects on the dynamics of a Rydberg electron: The residence time near the core

doi: 10.1063/1.480453

Magnetic field effects on the dynamics of a Rydberg electron: The residence time near the core

Hirohiko Kono,[a] Takayuki Tazaki, Isao Kawata, and Yuichi Fujimura
Department of Chemistry, Graduate School of Science, Tohoku University Sendai 980-8578, Japan

(Received 10 August 1999; accepted 29 September 1999)

Using symplectic integrator schemes, we calculate the classical trajectory of a Rydberg electron in external electric and magnetic fields. We also solve the equation of motion obtained by taking the mean values over one revolution of the electron in the undisturbed motion. The resulting secular motion is periodic. When only an electric field F is applied, as long as the modulation period in the orbital angular momentum l is longer than the revolution period, the motion agrees with the secular one and the duration for which l is much larger than its low initial value is stretched. The residence time (RT), namely, the probability of finding the electron at the distance r, is hence smaller than that at $F=0$. In crossed electric and magnetic fields, the secular motion predicts that an additional time stretching due to a magnetic field occurs up to the critical value of magnetic field strength, $B_c = 3\sqrt{3}nF$ (n is the principal action). In the actual simulations, the RT near the core is smaller than that at $B=0$ even beyond B_c, regardless of the magnitude of the non-Coulombic interaction C_2/r^2. Slow modulations in l are generated by transitions to secular motions that maintain high l, in addition to the fast modulation originating from the secular motion. When the magnetic field is so strong as to induce chaotic motion ($\sim$4000 G for the energy of -5 cm^{-1}), the RT is one order of magnitude as large as those in weak field cases around 40 G. In the intermediate region ($>$ a few hundred Gauss), without a non-Coulombic interaction, the RT monotonically increases as B increases. In the presence of C_2/r^2, transitions from low l states to high l states occur: the RT decreases. The motions in high l states can be explained by the well-known model in which an electron bound to the core by a harmonic force moves in a magnetic field. © *1999 American Institute of Physics.* [S0021-9606(99)00848-X]

I. INTRODUCTION

Experiments on the time-resolved decay of high Rydberg states of large molecules have shown that the decay has a major, sub μs, component and a smaller, μs-scale slow component.[1,2] The surviving Rydberg states can be detected using their ionization induced by a delayed field pulse known as zero kinetic energy.[3,4] High Rydberg states of atoms and molecules of rather low binding energies are susceptible even to weak external fields.[5–7] An external dc electric field modulates the value of the orbital angular momentum l of the Rydberg electron.[8,9] The distance of closest approach (perihelion distance) to the core, which is $l^2/2$ for $l/n \ll 1$ (n is the principal action), thereby also changes. An external electric field can periodically turn the coupling to the molecular core off and on. This causes an elongation of the decay times of Rydberg states.[10,11] Another possible intramolecular mechanism for long-time stability based on the sojourn in intermediate Rydberg states has been proposed by Rabani *et al.*[11]

When an external magnetic field that is perpendicular to the electric field is applied, the fraction of the slow decay component increases; an additional time stretching has been observed.[12] The Rydberg electron traces the orbit of a rather long semimajor axis: the motion is also altered even by the diamagnetic interaction of a weak magnetic field. Classical simulations have been performed for weak fields ($<$100 G for $n \approx 100$).[12] The role of the magnetic field in the weak field case may be summarized as follows. First, the angular momentum along the electric field axis, m_l, is not conserved when a magnetic field is applied in the direction not collinear with the electric field. Second, the diamagnetic term induces a slower modulation in l.

In this paper, we study magnetic field effects on the lifetime of the Rydberg electron from the viewpoint of the probability of finding the electron near the core (residence time). The residence time is used as a measure to quantify the interaction between the electron and the core. Classical simulations are performed by numerically stable symplectic integrator schemes,[13–15] up to a field intensity at which the motion is chaotic.[16] First, the effects of the Zeeman and diamagnetic terms in the weak field case are analyzed in terms of transitions among secular motions. Second, the residence time in the chaotic region is discussed. Finally, characteristic features in the intermediate regime of magnetic field strength are reported. In the intermediate regime, the residence time is drastically reduced by the joint effect of a magnetic field and a non-Coulombic interaction with the core.

II. MODEL AND METHOD

We first outline the model for a Rydberg electron in crossed electric and magnetic fields.[17,18] With the electric

[a]Electronic mail: kono@mcl.chem.tohoku.ac.jp

field F pointing in the z- and the magnetic field B pointing in the x-direction, the Hamiltonian in atomic units is

$$H = H_{\mathrm{magn}} - \frac{1}{r} + zF + K_{\mathrm{core}} + V_{\mathrm{core}} + V_{\mathrm{elec-core}}, \tag{1}$$

where K_{core} and V_{core} represent the kinetic and potential energies of the core, respectively, and $V_{\mathrm{elec-core}}$ represents the interaction between the electron and the core which leads to the quantum defect,[7] and H_{magn} is the Hamiltonian of the electron in the magnetic field

$$H_{\mathrm{magn}} = \frac{p_x^2 + p_y^2 + p_z^2}{2} + \frac{Bl_x}{2} + \frac{B^2}{8}(y^2 + z^2). \tag{2}$$

The unitless quantities given in this paper are measured in atomic units.

Recent classical, perturbative calculations have succeeded in explaining several diverse experimental results for the dynamics of Rydberg states. It has been shown that the expectation values of angular momentum and Runge–Lenz vectors in hydrogenic eigenstates obey exactly the same perturbative equations of motion as the time-averaged classical variables.[18] Here, the symplectic integrator (SI) method[13–15] is employed to solve Hamilton's equations of motion. We split the Hamiltonian into the following parts H_1 and H_2 which can be solved exactly when considered as independent Hamiltonians

$$H_1 = H_{\mathrm{magn}} + K_{\mathrm{core}}, \tag{3}$$

$$H_2 = -\frac{1}{r} + zF + V_{\mathrm{core}} + V_{\mathrm{elec-core}}. \tag{4}$$

The second-order SI, which is accurate through the second order of time spacing Δt, consists of three steps: (i) to obtain the solution at $\Delta t/2$ with H_1; (ii) to further evolve the system for Δt with H_2; (iii) to further evolve the system for $\Delta t/2$ with H_1. The solution at an arbitrary time can be obtained by repeating the three steps. The solution obtained leads to a symplectic map from the initial condition to the present state of the system (the Runge–Kutta schemes are not exactly symplectic). The system is thus kept from being damped or excited artificially. Because of this quality, SIs are applicable to long-time dynamics of Coulombic systems. The energy is conserved with astonishing accuracy. We perform numerical calculations up to a field intensity at which the motion is chaotic. In this paper, we use fourth- and sixth-order SI schemes composed of a product of second-order SIs.[13,15]

Rabani *et al.*[11,12] have solved Hamilton's equations of motion for the hydrogenic action variables by using a Gear six-order predictor–corrector method.[19] This method takes advantage of the fact that the action variables change little for a revolution of the electron around the core when the external fields are weak. For $B > 100\,\mathrm{G}$ (around $n = 100$), however, the integration of Hamilton's equations of motion is not numerically stable. As B increases, the value of n tends to change with larger amplitude.

In this paper, we report results in the absence of the internal degrees of freedom of the core, i.e., $K_{\mathrm{core}} = V_{\mathrm{core}} = 0$. The electron–core interaction is assumed to be represented by the non-Coulombic part of the spherically symmetric component of the potential as

$$V_{\mathrm{elec-core}} = \frac{C_2}{r^2}. \tag{5}$$

For this case, the angular momenta l_x, l_y, and l_z obey the following equations:

$$dl_x/dt = -yF, \tag{6a}$$

$$dl_y/dt = xF - Bl_z/2 + B^2xz/4, \tag{6b}$$

$$dl_z/dt = Bl_y/2 - B^2xy/4. \tag{6c}$$

In the absence of the non-Coulombic interaction, the equations of motion can be approximately solved by taking the mean values over one revolution of the electron in the undisturbed motion.[8,20] The resulting equations of motion, which provide periodic secular motions, are as follows:

$$d\bar{\mathbf{r}}/dt = (3n/2)^2 \mathbf{F} \times \mathbf{l} + \mathbf{B} \times \bar{\mathbf{r}}/2, \tag{7}$$

$$d\mathbf{l}/dt = \mathbf{F} \times \bar{\mathbf{r}} + \mathbf{B} \times \mathbf{l}/2, \tag{8}$$

where $\bar{\mathbf{r}}$ is the mean value of the position vector $\mathbf{r}$ and $\mathbf{l}$ is the angular momentum vector (since $\mathbf{l}$ is a slowly varying vector, the bars are dropped). Comparing Eqs. (6) and (8), one finds that in the secular motion model the effect of the diamagnetic term is completely eliminated. Introducing the frequency ω and the angle α,

$$\omega = [(3nF/2)^2 + (B/2)^2]^{1/2}, \tag{9}$$

$$\alpha = \tan^{-1}\frac{3nF}{B}, \tag{10}$$

we can express the secular motion with the period of $2\pi/\omega$ as

$$l_x(t) = (2/3n)\sin\alpha\left[-\bar{y}(0)\sin\omega t + 2\bar{z}(0)\cos\alpha\sin^2\frac{\omega t}{2}\right] + l_x(0)(\sin^2\alpha\cos\omega t + \cos^2\alpha), \tag{11a}$$

$$l_y(t) = (2/3n)\bar{x}(0)\sin\alpha\sin\omega t + l_y(0)\cos\omega t - l_z(0)\cos\alpha\sin\omega t, \tag{11b}$$

$$l_z(t) = (2/3n)\bar{x}(0)\sin 2\alpha\sin^2\frac{\omega t}{2} + l_y(0)\cos\alpha\sin\omega t + l_z(0)(\cos^2\alpha\cos\omega t + \sin^2\alpha), \tag{11c}$$

where the quantities with bars are their mean values over one initial period. The above equations are useful in analyzing the dynamics of a Rydberg electron on the basis of the secular motion model.

The interaction with the core can be quantified by the probability of finding the electron at r (the residence time) which is proportional to dt/dr. For the Kepler motion of angular momentum l, we know that[21]

$$\frac{dr}{dt} = \sqrt{(r_2 - r)(r - r_1)}/nr, \tag{12}$$

where r_1 is the periherion distance and r_2 the apherion distance. Using the eccentricity ε

$$\varepsilon=\sqrt{1-l^2/n^2}, \tag{13}$$

r_1 and r_2 are expressed as

$$r_1=n^2(1-\varepsilon), \tag{14}$$

$$r_2=n^2(1+\varepsilon). \tag{15}$$

Without an external field, the angular momentum l is conserved. If $l\ll n$, the residence time near the core per revolution of the electron is

$$\begin{aligned} R(r)=2dt/dr&\approx\sqrt{2r}/\sqrt{1-l^2/2r} \quad \text{for } r\geqslant l^2/2,\\ &=0 \quad \text{for } r<l^2/2. \end{aligned} \tag{16}$$

Since the trajectory passes the same r twice per revolution, dt/dr is multiplied by 2. Using the above result, as will be shown in the following section, one can analytically derive residence times in the presence of external fields.

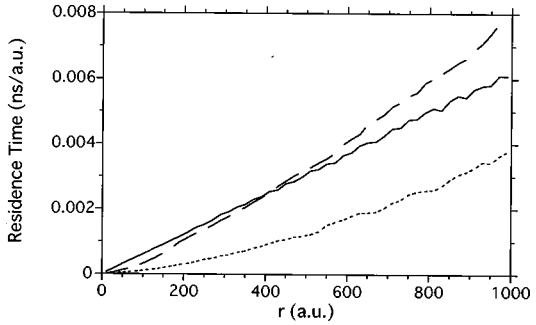

FIG. 1. Residence times calculated from 10 μs trajectory runs. The electric field strength is fixed at $F=0.1\ \mathrm{V\,cm^{-1}}$. The solid line represents the residence time at $B=0$ G. The broken and dotted lines represent the residence times at $B=40$ G for the first- and second-order cases, respectively. The initial condition is a $\theta=\pi/2$ case where $x=y=3.1\times10^4$ and $p_x=p_y=10^{-3}$ ($z=p_z=0$); $n\approx151$ (the total energy $E=-2.18\times10^{-5}$).

III. RESULTS AND DISCUSSION

A. Electric field effect

We first consider the effect of the secular motion of a Rydberg electron in an electric field. In this subsection, we set $B=C_2=0$. The angular momentum is very low just after excitation from a low electronic state to a high Rydberg state; we thus take the initial condition $l(0)=0$. We assume that the semimajor axis of the initial Kepler orbit is directed to polar coordinates θ and ϕ

$$\overline{x}(0)=\overline{r}(0)\sin\theta\cos\phi, \tag{17a}$$

$$\overline{y}(0)=\overline{r}(0)\sin\theta\sin\phi, \tag{17b}$$

$$\overline{z}(0)=\overline{r}(0)\cos\theta, \tag{17c}$$

where $\overline{r}(0)$ is the cycle average of the position projected onto the major axis

$$\overline{r}(0)=(3n^2/2)\sqrt{1-l^2(0)/n^2}. \tag{18}$$

Inserting Eqs. (17a)–(17c) into Eqs. (11), we can see that $l(t)$ depends on the azimuthal angle between the z-axis and the semimajor axis of the initial Kepler orbit, θ

$$l(t)=n|\sin\theta\sin\omega_0 t|, \tag{19}$$

where ω_0 is ω at $B=0$. The $l(t)$ modulates; it reaches $n|\sin\theta|$ and comes back to zero at intervals π/ω_0. The period of the secular motion in phase space is $2\pi/\omega_0\approx35$ ns for $n=150$ and $F=0.1$ V/cm.

Using Eq. (16), we can derive the residence time in the presence of an electric field. Suppose that the angular momentum for the orbit of the periherion distance r is l_c. If an orbit has an angular momentum less than l_c, the periherion distance is smaller than r; i.e., the orbits whose angular momentum are less than l_c contribute to the residence time $R(r)$. Assuming that the modulation period in l, π/ω_0, is longer than the revolution period $2\pi n^3$, i.e., $3n^4F<1$ (ionization due to barrier suppression sets a more severe condition $16n^4F<1$),[11] we take the following average:

$$R(r)=\int_0^{l_c}\frac{dt}{dr}P(l)dl. \tag{20}$$

The probability of taking l is normalized as

$$P(l)=\frac{dt}{dl}\Big/\int_0^{n|\sin\theta|}\frac{dt}{dl}dl=\frac{dt}{dl}\Big/(\pi/2\omega_0), \tag{21}$$

where dt/dl is given by

$$\frac{dt}{dl}=\frac{1}{\omega_0\sqrt{n^2\sin^2\theta-l^2}}. \tag{22}$$

For the secular motion in an electric field, $R(r)$ in Eq. (20) is independent of F.

For an orbit that can come close to the core, $l\ll n$. In this case, dt/dr is given by Eq.(16). We finally obtain

$$\begin{aligned} R(r)&=\frac{4r}{n\pi|\sin\theta|}K\left(\frac{\sqrt{2r}}{n\sin\theta}\right) \quad \text{for } r<\frac{n^2\sin^2\theta}{2}\\ &=\frac{2\sqrt{2r}}{\pi}K\left(\frac{n\sin\theta}{\sqrt{2r}}\right) \quad \text{for } r>\frac{n^2\sin^2\theta}{2}, \end{aligned} \tag{23}$$

where K is the complete elliptic integral of the first kind. When $r\ll(n\sin\theta)^2/2$ (this is valid for $n=150$ and $r<10^3$),

$$R(r)\approx2r/n|\sin\theta|, \tag{24}$$

which increases linearly with r.

The residence time for $F=0.1\ \mathrm{V\,cm^{-1}}$ and $n\approx151$ (total energy $E\approx-2.18\times10^{-5}$) calculated from a trajectory run is shown by the solid line in Fig. 1. The initial condition is a $\theta=\pi/2$ case where $x=y=3.1\times10^4$ and $p_x=p_y=10^{-3}$($z=p_z=0$). The trajectory runs for 10 μs. For a weak field like in the present case, the secular motion is maintained. The accumulated residence time is related with $R(r)$ in Eq. (24) as

Accumulated residence time

$$=\frac{\text{run time of the trajectory}}{\text{period of the revolution}}R(r). \tag{25}$$

The result of the simulation agrees with Eq. (25). As long as $3n^4F\ll1$, the secular motion is maintained and the time in which the electron has high angular momenta is stretched in

comparison with the $F=0$ case (called the time stretching[11]); the residence time accumulated for a time much longer than π/ω_0 is independent of F.

B. Secular motion in crossed electric and magnetic fields

We again in Eqs. (11a)–(11c) assume that $l(0)=0$. When $B\neq 0$, $\alpha\neq\pi/2$: l_x and l_z can have components that change as $\sin^2(\omega t/2)$. The period of taking $l=0$ is then doubled; i.e., $l\neq 0$ at $t=\pi/\omega$, unlike the case where only an electric field is applied (the $B=0$ case). The increase and decrease in l near $l=0$ (which occur with a period of $2\pi/\omega$) are governed by the term $\sin\alpha\sin\omega t$ in the l_x and l_y components which exhibits the same increase or decrease of l in the $B=0$ case

$$\sin\alpha\sin\omega t\approx(3nF/2)t. \tag{26}$$

The way of approaching and leaving the core when l is small is thus independent of B. The $\sin^2(\omega t/2)$ components in l_x and l_z rise later because they increase as $(3nFB/4)t^2$. For a fixed time span, the time in which the electron has high angular momenta is further stretched by a magnetic field B if the modulation period is longer at B than at $B=0$

$$2\pi/\omega>\pi/\omega_0. \tag{27}$$

The modulation period is defined as $2\pi/\omega$ for $B\neq 0$, while it is defined as π/ω_0 for the $B=0$ case. The inequality (27) means that $B<B_c$, where the critical value is defined as $B_c\equiv 3\sqrt{3}nF$.

Another factor to determine the interaction with the core is how high the quantity l can go. As an example, we take the case that $\overline{x}(0)\neq 0$ and $\overline{y}(0)=\overline{z}(0)=0$. If $\alpha\geqslant\pi/4$, i.e., $3nF/B\geqslant 1$, two peaks whose heights are n exist in a modulation period $2\pi/\omega$. The height at $t=\pi/\omega$, l_{middle}, which corresponds to the bottom of the middle valley between the two peaks, is given by $n\sin 2\alpha$. For $\alpha<\pi/4$, l has only one peak, of which height l_{middle} is also given by $n\sin 2\alpha$. We have to compare $l_{\mathrm{middle}}(=n\sin 2\alpha)$ with a threshold value below which strong interaction with the core is expected, l_{th}. As long as $l_{\mathrm{middle}}\gg l_{\mathrm{th}}$, Eq. (26) holds: the time duration in which $l(t)<l_{\mathrm{th}}$ is $\sim 2l_{\mathrm{th}}/F\overline{x}(0)$ per modulation period for l, which is independent of B. Since, in comparison with l_{th}, l_{middle} is expected to be high enough at $B=B_c$ (at which $n\sin 2\alpha=\sqrt{3/4}n\approx n$), an additional time stretching occurs up to B_c. For $n=150$ and $F=0.1\,\mathrm{V\,cm^{-1}}$, B_c amounts to 35 G.

We can extend the above discussion by including an initial distribution in phase space. We assume that the initial state is ns (for which $l=0$). The isotropic initial distribution in configuration space can be expressed using Eqs. (17a)–(17c). Angle variables θ and ϕ are distributed isotropically. The average of $l^2(t)$ is given by

$$\langle l^2(t)\rangle=(n\sin\alpha)^2\left(8\sin^2\omega t+36\cos^2\alpha\sin^4\frac{\omega t}{2}\right)\Big/15. \tag{28}$$

The increase and decrease near $l=0$ are again independent of B

$$\sqrt{8}n\sin\alpha\sin\omega t\approx\sqrt{8}n(3nF/2)t. \tag{29}$$

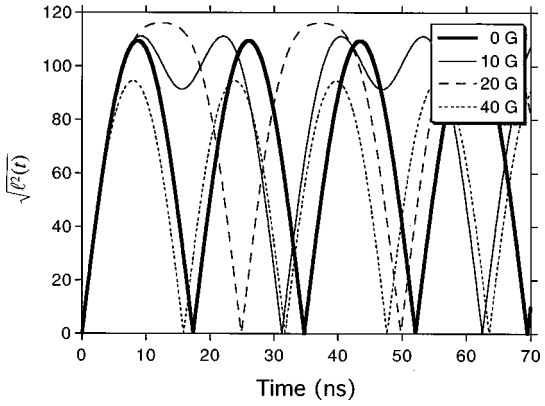

FIG. 2. The averaged magnitude of angular momentum, the square root of Eq. (28), for secular motions at four different magnetic field strengths ($n=150$ and $F=0.1\,\mathrm{V\,cm^{-1}}$). The initial positions are assumed to be isotropically distributed.

The $\sqrt{\langle l^2(t)\rangle}$ is plotted in Fig. 2 for different magnetic field strengths ($n=150$ and $F=0.1\,\mathrm{V\,cm^{-1}}$). For $0<\cos\alpha<2/3$ (i.e., $B<3\sqrt{4/5}nF$), as shown by the thin solid line in Fig. 2, two peaks exist in a modulation period $2\pi/\omega$. In this case, the peak height l_{max} is

$$l_{\mathrm{max}}=n\left[\left(\frac{8}{15}\right)\left(1+\frac{\cos^2\alpha}{8-9\cos^2\alpha}\right)\right]^{1/2}, \tag{30}$$

and the bottom of the middle valley is given by

$$l_{\mathrm{middle}}=n\sqrt{9/15}\sin 2\alpha. \tag{31}$$

For $\cos\alpha<2/3$, l_{max} exceeds the value at $B=0$, $l_{\mathrm{max},0}\equiv n\sqrt{8/15}$. For $\cos\alpha>2/3$, the bottom of the valley becomes the peak. As in the case of starting from $\overline{x}(0)\neq 0$, the time stretching due to a magnetic field requires that $2\pi/\omega>\pi/\omega_0$ (as shown in Fig. 2, this condition is fulfilled below $B=35\,\mathrm{G}$). At the critical intensity B_c, l_{middle} is as high as $l_{\mathrm{max},0}$; $l_{\mathrm{middle}}=\sqrt{27/32}l_{\mathrm{max},0}\approx l_{\mathrm{max},0}$. The secular motion model predicts that an additional time stretching due to a magnetic field occurs up to the critical intensity.

The residence time is related to that for $B=0$, $R_0(r)$, as

$$R(r)\approx\frac{\omega}{2\omega_0}R_0(r), \tag{32}$$

where we have considered that the increase and decrease near $l=0$ are independent of B and the number of times of taking $l=0$ is proportional to $\omega/2\omega_0$. The minimum of this factor is 1/2 for $B=0$. However, when B is as small as $\omega/2\omega_0\approx 1/2$, $l_{\mathrm{middle}}<l_{\mathrm{th}}$; the residence time is supposed to be as large as $R_0(r)$. A finite magnetic field strength is required for the onset of the additional time stretching.

C. First- and second-order effects of weak magnetic fields

In the above subsection, we have discussed the effect of the secular motion on the time stretching in the presence of a magnetic field. Here, the first- and second-order effects of magnetic fields are considered. In this paper, when the Zeeman term is included but the diamagnetic term is dropped,

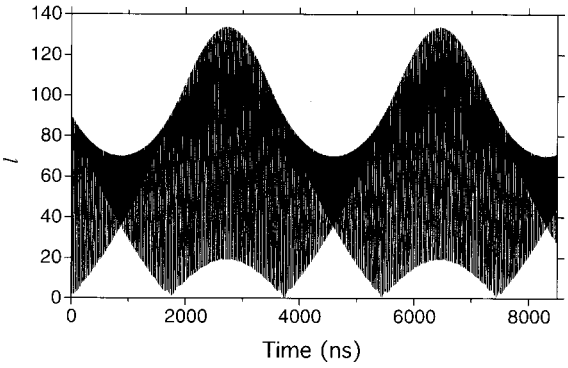

FIG. 3. A first-order field effect on l for $B=40$ G and $F=0.1$ V cm^{-1}. The initial condition for the trajectory is the same as in Fig. 1.

the effect is referred to as the first-order one; when both terms are included, the effect is referred to as the second-order one.

The broken and dotted lines shown in Fig. 1 are the residence times for the first- and second-order cases at $B=40$ G, respectively. The initial condition is the same as the $B=0$ case in Fig. 1. Since $\omega/2\omega_0 \approx 1.1$ for $B=40$ G ($>B_c$), the residence time based on the secular motion is larger than that at $B=0$. On the other hand, the residence time for the first-order case, which has a quadratic component with r, is smaller than that at $B=0$ up to $r\approx 400$. The change in l for the first-order case is drawn in Fig. 3. A slow modulation with a period of 3700 ns is observed, in addition to the fast modulation originating from the secular motion ($2\pi/\omega=16$ ns). The slow modulation is responsible for the reduction in the residence time for $r<400$.

As shown by the dotted line in Fig. 1, the residence time is drastically reduced in the second-order case. It should be noted that the residence time increases quadratically with r. The change in l is drawn in Fig. 4. In addition to the fast modulation, l modulates with a longer period of 200 ns (The period in the phase space is the double.) The period of the slow modulation is much shorter than in the first-order case.

The residence times for $B=20$ G are shown in Fig. 5. This intensity satisfies the condition $B<B_c$. In both the first- and second-order cases, the ratio of the residence time to that at $B=0$ G, $R(r)/R_0(r)$, is smaller at $B=20$ G than that at 40 G. The period of the slow modulation is longer than at 40 G.

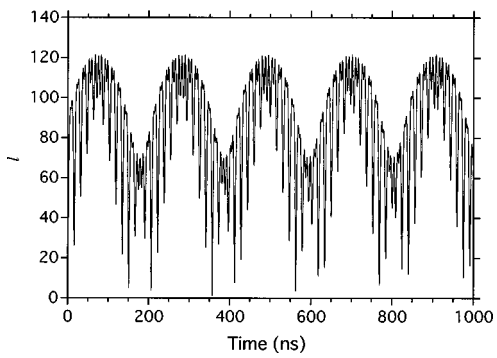

FIG. 4. A second-order field effect on l for $B=40$ G and $F=0.1$ V cm^{-1}. The initial condition for the trajectory is the same as in Fig. 1.

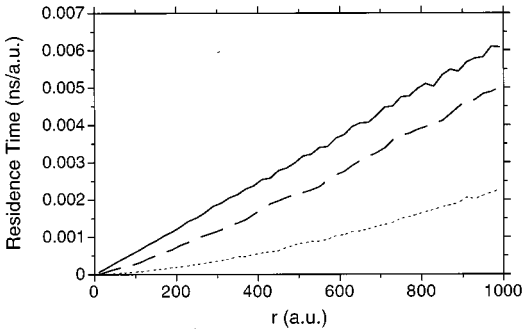

FIG. 5. Residence times calculated from 10 μs trajectory runs. The solid line represents the residence time at $B=0$ G. The electric field strength is fixed at $F=0.1$ V cm^{-1}. The broken and dotted lines represent residence times at $B=20$ G for the first- and second-order cases, respectively. The initial condition for the trajectories is the same as in Fig. 1.

It is concluded that $R(r)/R_0(r)$ in the second-order case is much smaller than the ratio $\omega/2\omega_0$ predicted by the secular motion model ($\omega/2\omega_0\approx 0.7$ at 20 G).

When non-Coulombic interactions with the core are present, the Rydberg electron precesses. If the precession is very rapid, it counteracts the effect of the fields. For the non-Coulombic term C_2/r^2, the period of the precession is given by

$$T_{\mathrm{pre}}=2\pi n^3 l^2/C_2. \tag{33}$$

If the motion is a secular type, the increase in l from $l=0$ is governed by

$$l\approx n\sin\alpha\sin\theta\sin\omega t|\approx|\sin\theta|(3n^2F/2)t, \tag{34}$$

which is nearly independent of B. The time required to reach l_{th} is

$$T_{\mathrm{th}}\approx 2l_{\mathrm{th}}/|3n^2F\sin\theta|. \tag{35}$$

If $T_{\mathrm{th}}>T_{\mathrm{pre}}$, i.e.,

$$\frac{3\pi n^5 l^2 F\sin\theta}{C_2 l_{\mathrm{th}}}<1, \tag{36}$$

the precession changes the residence time, i.e., it affects the interaction with the core. The precession is operative only when l is small.

Generally speaking, l starts increasing from a configuration around $\theta=\pi/2$. The precession hinders the increase in l: the residence time near the core increases with decreasing precession period up to a saturation level. For the secular motion case, from Eq. (36), we notice that the effect of the precession per l-modulation period is nearly independent of B. Since the number of times of taking small l for an overall run is then proportional to $\omega/2\omega_0$, the net effect of the precession is also proportional to $\omega/2\omega_0$. In comparison with the $B=0$ case, therefore, the residence time would be smaller up to B_c and increases as B increases beyond B_c.

Numerical examples for $C_2=0.3$ are presented in Figs. 6 and 7 ($F=0.1$ V cm^{-1}). The first-and second-order results at $B=20$ G are shown in Fig. 6 and those at 40 G are shown in Fig. 7. The present non-Coulombic interaction increases the residence time at $B=0$ by 50% (cf. the solid lines in Figs. 5 and 6). The first-order results are in accord with those pre-

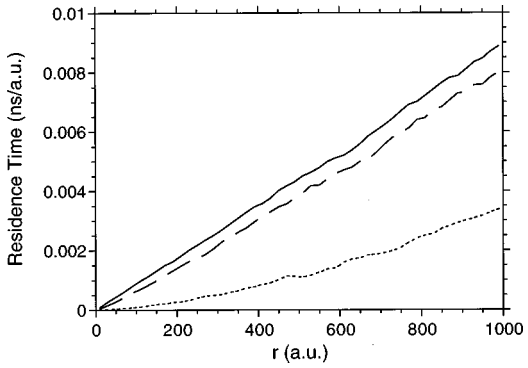

FIG. 6. Residence times at $B=20$ G in the presence of the non-Coulombic interaction. The interaction strength and the electric field are fixed as $C_2=0.3$ and $F=0.1$ V cm^{-1}. The notations are the same as in Fig. 5.

dicted by the secular motions; when $B<B_c=35$ G, the residence time is smaller than that at $B=0$, and when $B>B_c$, the residence time is larger. When $C_2>0.2$ for $B=20$ G ($C_2>0.25$ for $B=40$ G), in the first-order case, the slow modulation observed as in Fig. 3 disappears; the l modulates as fast as in the secular motion case with the frequency ω. While the first-order effect is susceptible to non-Coulombic interactions, as shown in Figs. 6 and 7, the second-order effect is robust. *Even for unphysically large values of* C_2, *the residence time in the second-order case is smaller than that at* $B=0$ and the quadratic increase with r remains because slow modulations still exist. The second-order effect appears except when $x=0$. In the case where $x=0$, the second-order effect is minimized as predicted from Eq. (6).

The slow modulations can be described by transitions among secular motions. As an example, the positions and angular momenta for the second-order case of $B=40$ G and $C_2=0.3$ are plotted in Figs. 8 and 9, respectively. As observed, in a short time scale, a periodic motion of high angular momentum is maintained ($60<l<120$). The periodic motion in Fig. 8 is a typical one when l is high. This transient ''periodic'' motion is described by Eq. (11) for the secular motion. The initial time $t=0$ in Eq. (11) should be replaced with an intermediate time at which a transient periodic motion is defined, t_0; then, $\overline{x}(0)$, $\overline{y}(0)$, $\overline{z}(0)$, $l_x(0)$, $l_y(0)$, and $l_z(0)$ should be replaced with $\overline{x}(t_0)$, $\overline{y}(t_0)$, $\overline{z}(t_0)$, $l_x(t_0)$, $l_y(t_0)$, and $l_z(t_0)$, respectively. The time t on the right-hand

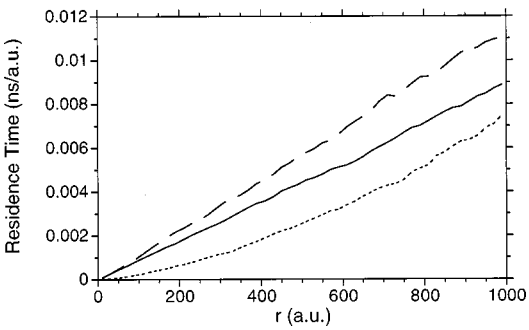

FIG. 7. Residence times at $B=40$ G for the first- and second-order cases in the presence of the non-Coulombic interaction ($C_2=0.3$ and $F=0.1$ V cm^{-1}). The notations are the same as in Fig. 5.

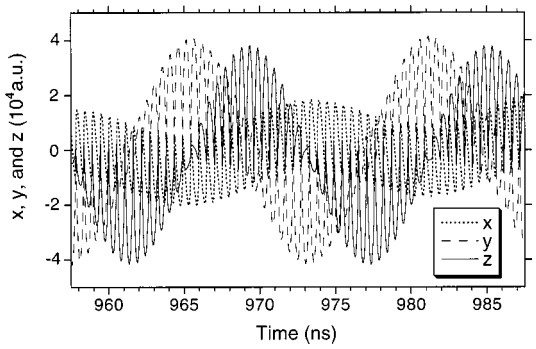

FIG. 8. Change in positions for $B=40$ G and $C_2=0.3$ ($F=0.1$ V cm^{-1}).

side of Eq. (11) is measured from t_0. The choice of t_0 is rather arbitrary. A convenient way to prove the existence of transient secular motions is to choose a time t_0 so that $\overline{z}(t_0)=0$. Then, the other two parameters $\overline{x}(t_0)$ and $\overline{y}(t_0)$ can be easily determined from

$$\overline{x}(t_0)=\frac{3n}{2\sin\alpha}\left[l_y\left(t_0+\frac{\pi}{2\omega}\right)+l_z(t_0)\cos\alpha\right], \tag{37}$$

$$\overline{y}(t_0)=\frac{3n}{2\sin\alpha}\left[l_x(t_0)\cos^2\alpha-l_x\left(t_0+\frac{\pi}{2\omega}\right)\right]. \tag{38}$$

For instance, from Fig. 8, we can set $t_0=965.39$ ns: from Fig. 9, $l_x(t_0)=-16.37$, $l_y(t_0)=-1.58$, and $l_z(t_0)=67.06$; at $t_0+\pi/2\omega=969.35$ ns, $l_x(t_0+\pi/2\omega)=-73.04$, $l_y(t_0+\pi/2\omega)=-82.39$. We thus obtain $\overline{x}(t_0)=-11250$ and $\overline{y}(t_0)=29\,630$. The secular motion determined by the six parameters at t_0 perfectly fits the result in Fig. 9.

A tabular summary of the findings in Secs. III B and III C is given in Table I.

D. Strong magnetic field and intermediate cases

Results for $B=4000$ G are shown in Fig. 10. The residence time is one order of magnitude as large as those presented so far. Much stronger interaction with the core is expected. The residence time is not as sensitive to the non-Coulombic interaction (and to F).

It should be noted that the residence time increases linearly with r, unlike in the second-order cases for $B=20$ or 40 G. For the present strong magnetic field, the motion is extensively chaotic.[16] The electron comes close to the core in a

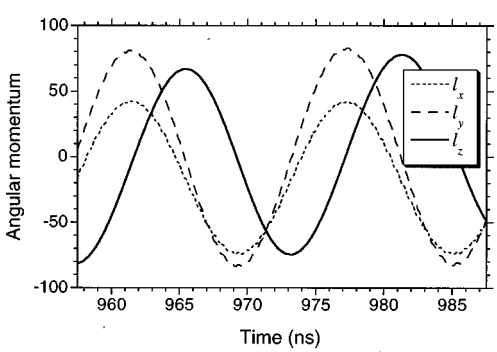

FIG. 9. Change in angular momenta for $B=40$ G and $C_2=0.3$ ($F=0.1$ V cm^{-1}).

TABLE I. Criteria for the additional time stretching due to a magnetic field B. The mechanism of the time stretching is twofold. One is the secular motion effect which increases the effective period of the fast modulation in l. The other mechanism originates from slow modulations in l which are induced by transitions among secular motions. The presence of the fast and slow modulations is designated by the abbreviations F and S. The critical magnetic field strength B_c is defined as $3\sqrt{3}n\times$(electric field strength).

	$C_2=0$ case	$C_2\neq 0$ case
Secular motion effect	$B<Bc$ (F)	$B<Bc$ (F)
First-order effect	$B<$a few times Bc (F+S)	$B<Bc$ (F)
Second-order effect	$B<$severaltimes Bc (F+S)	$B<$several times Bc (F+S)

chaotic manner (on the average, the angular momentum l changes faster than the radial distance r). Combining this fact with the effective Hamiltonian near the core,

$$\frac{1}{2}(p_x^2+p_y^2+p_z^2)-\frac{1}{r}=E. \tag{39}$$

one can assume that the electron randomly appears on the isoenergetic surface in momentum space which forms a sphere of radius $\sqrt{2}(E+1/r)^{1/2}$. The surface area of the sphere is $8\pi(E+1/r)$. Taking into account the volume element in polar coordinates $r^2\sin\theta dr\,d\theta\,d\phi$, we find that

$$R(r)\propto 8\pi(E+1/r)r^2. \tag{40}$$

For $E\ll 1/r$, $R(r)\propto r$ (this is the case for $E\approx -2.18\times 10^{-5}$ and $r\approx 10^3$).

We finally summarize characteristic features in the intermediate regime. Around $B=600$ G, the residence time for the second-order case is proportional to r and is on the level of 0.01 at $r=1000$. When $C_2=0$, the residence time monotonically increases as B increases further; for example, the residence time for $B=2000$ G is as large as in Fig. 10 for $B=4000$ G. In the 2000 G case, however, when a nonzero value is set for C_2, the residence time decreases below the level for $B=600$ G and a quadratic component with r appears. This type of reduction in the residence time is induced by transitions from low l states to high l states due to the non-Coulombic interaction.

A typical high l state for $B=2000$ G and $C_2=0.3$ is shown in Fig. 11. The initial condition is that $x=y=1.568\times 10^4$ and $p_x=p_y=10^{-3}$ ($E=-2.18\times 10^{-5}$). For the time region shown in Fig. 11, l_x is between -160 and -170 and $l\geqslant 200$. The fast oscillation with a period of $\sim$0.16 ns is superimposed on the slow oscillation with a period of $\sim$2 ns. The motion cannot be fitted by the secular model. The most suitable one is the well-known model in which an electron bound to the core by a harmonic force $-k\mathbf{r}$ moves in a magnetic field

$$d^2\mathbf{r}/dt=-k\mathbf{r}-\mathbf{v}\times\mathbf{B}. \tag{41}$$

For $B_x=B\neq 0$ and $B_y=B_z=0$, the electron rotates around the x-axis while moving back and force along the x-axis. The rotation consists of the fast and slow modes ω_f and ω_s whose frequencies are given by

$$\omega_f=\frac{B}{2}+\sqrt{k+\left(\frac{B}{2}\right)^2}. \tag{42a}$$

$$\omega_s=\frac{B}{2}-\sqrt{k+\left(\frac{B}{2}\right)^2}. \tag{42b}$$

The ω_s is negative, which corresponds to the rotation in the direction opposite to the cyclotron motion. If the Coulomb potential is fitted to a harmonic one, we have $k=1/r^3$. For the range shown in Fig. 11, the average of r is about 2.5×10^4. From Eq. (42), we obtain $2\pi/\omega_f=0.16$ ns and $2\pi/|\omega_s|=2.2$ ns. These two frequencies agree with those observed in Fig. 11. As the average of r is larger, $|\omega_s|$ becomes smaller.

Before closing this section, we would like to mention the accuracy of our numerical results. The trajectories in Secs. III A and C are quasiperiodic. In this regime, the fourth- and sixth-order SIs provide trajectories that are reliable for long time dynamics; convergence is reached by reducing variable time spacings. On the other hand, in the near chaotic and chaotic regimes as in this subsection, the trajectory is unstable with the change in time spacings. However, the quantity that we concentrate on, namely, the residence time for a long run, is insensitive to the details of the trajectory. We assume that the errors of a trajectory cancel out in the long time average of the residence time.

Schlier and Seiter[22] have examined classical trajectories for a triatomic, complex forming system and have already demonstrated the limitation of symplectic integration. In the chaotic regime, neither stable conservation of phase volume

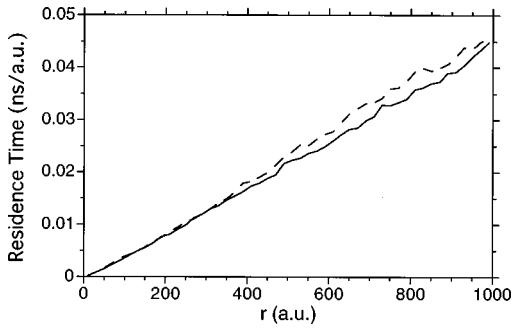

FIG. 10. Residence times at $B=4000$ G ($F=0.1$ V cm^{-1}). The solid and broken lines represent the residence times for $C_2=0.3$ and $C_2=0$, respectively. The initial condition is as follows: $x=y=1.083\times 10^4$ and $p_x=p_y=10^{-3}$ ($E=-2.18\times 10^{-5}$).

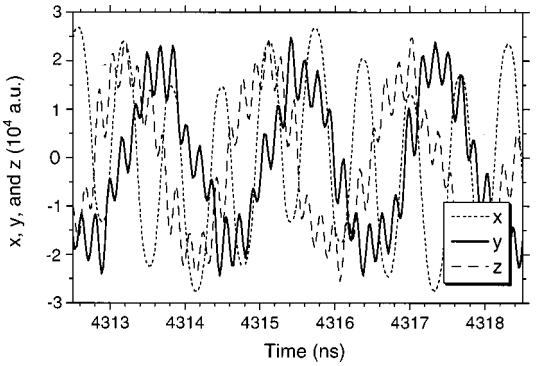

FIG. 11. Change in positions for a typical high angular momentum state at $B=2000$ G and $C_2=0.3$ ($F=0.1$ V cm^{-1}). The initial condition is that $x=y=1.568\times 10^4$ and $p_x=p_y=10^{-3}$ ($E=-2.18\times 10^{-5}$).

nor good energy conservation guarantee that the trajectory is correct, or even that it reaches the correct reaction channel. This defect may lead to wrong conclusions when it takes a long time to arrive at a rarely populated channel. In this case, it is difficult to obtain a sufficient number of long-lived trajectories. We face the same problem when the internal degrees of freedom of the core are included, i.e., autoionization channels are open. Extra caution must be exercised on the study of autoionization in the chaotic regime.

IV. SUMMARY AND CONCLUSIONS

Using fourth- and sixth-order symplectic integrator schemes, we have calculated the classical dynamics of a Rydberg electron in crossed electric and magnetic fields. Numerical calculations have been performed up to a field intensity at which the motion is chaotic. In this paper, we report results in the absence of the internal degrees of freedom of the core.

The equations of motion can be approximately solved by taking the mean values over one revolution of the electron in the undisturbed motion. Our starting point is the secular motion, i.e., the periodic solution of the approximate equation of motion. When only an electric field is applied, as long as the modulation period in the orbital angular momentum l, $\pi/\omega_0 \equiv \pi/(3nF/2)$, is longer than the revolution period $2\pi n^3$, i.e., $3n^4F \ll 1$, the motion agrees with the secular motion; the residence time accumulated for a time much longer than π/ω_0 is independent of F. The electric field stretches the duration for which the angular momentum is much larger than its initial value and reduces the interaction with the core. In crossed electric and magnetic fields, the secular motion predicts that an additional time stretching due to magnetic field occurs up to the critical intensity of magnetic field, $B_c = 3\sqrt{3}nF$. Within the framework of the secular motion model, the residence time near the core increases linearly with r.

In the numerical simulations beyond the secular motion model, the residence time near the core has a quadratic component with r and is smaller than that at $B=0$ even beyond B_c, *even for unphysically large values of* C_2 in the non-Coulombic interaction C_2/r^2. Slow modulations in l are observed, in addition to the fast modulation originating from the secular motion. The slow modulations are interpreted as transitions to secular motions that maintain high values of l. The diamagnetic term plays the major role in slow modulations.

When the magnetic field is so strong as to induce chaotic motion extensively, much stronger interaction with the core is expected. When the energy is about -2×10^{-5}, the residence time at 4000 G is one order of magnitude as large as those around 40 G. The residence time increases linearly with r; the quadratic increase with r disappears.

In the intermediate region, without a non-Coulombic interaction, the residence time monotonically increases as B increases ($>$ a few hundred Gauss). In the presence of the non-Coulombic interaction, the residence time at 2000 G decreases below the level at 600 G and a quadratic component with r appears. This is induced by transitions from low l states to high l states due to the non-Coulombic interaction. The motions in high l states can be explained by the well-known model in which an electron bound to the core by a harmonic force $-\mathbf{r}/\langle r^3\rangle$ moves in a magnetic field.

ACKNOWLEDGMENTS

This work was supported in part by the Department of High-Density Optical Pulse Generation and Advanced Material Control Techniques. We wish to thank Dr. H. Umeda and Dr. A. Fujii for valuable discussion. We would also like to express our appreciation to Dr. H. Yoshida for allowing us to consult SI schemes for the Kepler problem.

[1] D. Bahatt, U. Even, and R. D. Levine, J. Chem. Phys. **98**, 1744 (1993).
[2] U. Even, R. D. Levine, and R. Bersohn, J. Phys. Chem. **98**, 3472 (1994).
[3] K. Müller-Dethlefs and E. W. Schlag, Annu. Rev. Phys. Chem. **42**, 109 (1991); E. W. Schlag, *ZEKE Spectroscopy* (Cambridge University Press, Cambridge, 1998); K. Müller-Dethlefs and M. C. R. Cockett, in *Nonlinear Spectroscopy for Molecular Structure Determination*, edited by R. W. Field, E. Hirota, J. P. Maier, and S. Tsuchiya (Blackwell Science, Bodmin, 1998).
[4] D. P. Taylor, J. G. Goode, J. E. LeClaire, and P. M. Johnson, J. Chem. Phys. **103**, 6293 (1995).
[5] *Rydberg States of Atoms and Molecules*, edited by R. F. Stebbings and F. B. Dunning (Cambridge University Press, Cambridge, 1983).
[6] T. F. Gallagher, *Rydberg Atoms* (Cambridge University Press, Cambridge, 1994).
[7] J-.P. Connerade, *Highly Excited Atoms* (Cambridge University Press, Cambridge, 1998).
[8] W. Pauli, Z. Phys. **36**, 3369 (1926).
[9] M. Born, *Mechanics of the Atom* (Blackie, London, 1951), Chap. 3.
[10] W. A. Chupka, J. Chem. Phys. **98**, 4520 (1993).
[11] E. Rabani, R. D. Levine, A. Mühlpfordt, and U. Even, J. Chem. Phys. **102**, 1619 (1995).
[12] A. Mühlpfordt, U. Even, E. Rabani, and R. D. Levine, Phys. Rev. A **51**, 3922 (1995).
[13] H. Yoshida, Phys. Lett. A **150**, 262 (1990).
[14] H. Yoshida, Celest. Mech. Dyn. Astron. **56**, 27 (1993).
[15] E. Forest and R. D. Ruth, Physica D **43**, 105 (1990).
[16] H. Hasegawa, M. Robnik, and G. Wunner, Suppl. Prog. Theor. Phys. **98**, 198 (1989); H. Ruder, G. Wunner, H. Herold, and F. Geyer, *Atoms in Strong Magnetic Fields* (Springer, Berlin, 1994).
[17] K. Weibert, J. Main, and G. Wunner, Ann Phys. (N.Y.) **268**, 172 (1998).
[18] P. Bellomo, C. R. Stroud, Jr., D. Farrelly, and T. Uzer, Phys. Rev. A **58**, 3896 (1998).
[19] C. W. Gear, *The Numerical Integration of Ordinary Differential Equations of Various Orders*, Report ANL 7126, Argonne National Laboratory, 1966.
[20] Secs. 37 and 38 in Ref. 9.
[21] L. D. Landau and E. M. Lifshitz, *Mechanics*, 3rd ed. (Pergamon, Oxford, 1976), Sec. 15.
[22] Ch. Schlier and A. Seiter, J. Phys. Chem. A **102**, 9399 (1998).